Available online at www.sciencedirect.com
SCIENCE DIRECT®
Polymer 45 (2004) 1689–1696
polymer
www.elsevier.com/locate/polymer

Intrafibrillar bridging structures in strained isotactic polypropylene

Katherina Tsobkallo[a], A. Tikhomirov[a], A. Tshmel[b,*]

[a]St. Petersburg State University of Technology and Design, B. Morskaya 18, 191185 St. Petersburg, Russian Federation
[b]Fracture Physics Department, Ioffe Physico-Technical Institute, Russian Academy of Sciences, Polytechnicheskaya, 26, 194021 St. Petersburg, Russian Federation

Received 18 July 2003; received in revised form 8 December 2003; accepted 18 December 2003

Abstract

The films made of isotactic polypropylene were strained up to 0.8 of their ultimate strain and subjected to isometric stress relaxation during 5 days. The strain–stress curves were measured at various stages of the sample treatment and the tangent moduli (E_t) of unstrained, as-strained and relaxed films were determined. The changes of values of E_t were put in comparison with the structural evolution of strained samples observed using the infrared and low-frequency Raman spectroscopic techniques. It was concluded that the three-dimensional intercrystallite bridges composed of straight-chain segments of lengths $L_c < L < 2L_c$ (L_c is the average thickness of crystallites) destruct as a result of chain-breaking process, but due to the chain-straightening events in isometrically relaxing samples, the intercrystallite space transforms to the rigid amorphous phase composed of 'individual' one-dimensional molecular stems.

Keywords: Isotactic polypropylene; Tangent modulus; LAM

1. Introduction

The mechanical properties of semicrystalline polymers are determined by a set of their morphological characteristics related to the natural heterogeneity of these materials. In order to establish the main mechanical-structural correlations, that is to distinguish the structural features that govern the elastoplastic response of a given semicrystalline polymer, and vice versa, to trace the structural changes induced by the strain/stress effects, number of studies has been performed during the last decade. As regards the isotactic polypropylene (i-PP) [1], a great part of works has been devoted to unoriented [2–4], or weakly oriented polypropylenes (such as compression-mould [5–7] and injected-mould [8,9] materials). This preference is partially caused by remarkable mechanical properties of low-oriented i-PP (high stiffness and tensile stress) while the oriented i-PP goes behind oriented polyethylene (PE) which is widely extended in the form of drawn fibers and films. At the same time, the morphology of highly oriented i-PP is close to that of PE [7] what allows one to use common models of the structure-mechanics interconnection developed for semicrystalline polymers [10,11]. However, one can expect that very low value of the Young's modulus of pliable helical macromolecules (~ 40 GPa [12] against ~370 GPa in PE [13]) in combination with the initial structural complexity of i-PP (to mention cross-hatching [14] and great difference in the mechanical response of spherulites belonging to different crystallographic forms [4]) would introduce some specific features in mechanical behavior of oriented i-PP samples.

In order to elucidate some specific properties of highly oriented i-PP, in this work we studied in situ the structural response (i.e. chain-breakage and chain-straightening) in drawn films subjected to loading with subsequent stress relaxation.

In general, the stress-induced bond ruptures, on the one hand, and the chain straightening, on the other hand take place predominantly in the 'non-crystalline' (intercrystallite and interfibrillar) regions and, from the viewpoint of their effect on the mechanical properties of a sample, should be regarded as competitive. Chain straightening leads to formation of more rigid molecular structure with corresponding increase of the tangent modulus, while the bond ruptures reduce the connectivity of the molecular network

* Corresponding author. Tel.: +7-812-2479139; fax: +7-812-2478924.
E-mail address: alex@ac7773.spb.edu (A. Tshmel).

0032-3861/$ - see front matter © 2003 Elsevier Ltd. All rights reserved.
doi:10.1016/j.polymer.2003.12.054

with decreasing both the tangent modulus and strength of the polymer.

The straight chain segments (SCS) in i-PP manifest themselves in the low-frequency Raman spectrum by the band of longitudinal acoustic modes (LAM) localized in helical macromolecules [15]. The observed changes in the SCS length distribution were put in comparison with the changes of the tangent modulus.

The data on the bond-breaking process in strained samples were obtained from the IR spectroscopic measurements.

2. Experimental

2.1. Samples and mechanical tests

The samples were commercial i-PP films 63–68 μm thick with draw ratio (λ) equal to 15. Molecular weight (M_W) of the polymer was 2×10^5 a.u. In order to obtain the structural response from the samples with different thermal prehistory, a reference film was treated in the thermostat at 130 °C during 3 h. A shrinkage ratio after this annealing procedure was about 6%. All the instrumental experiments were carried out at the room temperature.

The mechanical tests were performed on a universal Instron 1122 Tensile Tester. The strain rate was 50 mm/s.

2.2. IR spectroscopy

The IR experiments were carried out on a Perkin–Elmer Fourier spectrometer Model 'Spectrum One' in a transmission mode. The changes in broken bond concentration in stressed films were estimated from the intensities of the selective IR bands at 1640 and 1742 cm^{-1}, belonging to the chemical groups $-CH{=}CH_2$ and $-CH_2-CH{=}O$, respectively [4]. These groups are secondary products of polymer decomposition; they emerge after decay of primary short-life radicals formed on the ends of broken macromolecules of i-PP. The number of chain breaks is proportional to the Lambert–Beer coefficient, α, of corresponded bands: $\alpha = \log(I/I_0)/d$, where I and I_0 are the intensities of the incident IR radiation and transmitted through the sample of thickness d.

2.3. Low-frequency Raman spectroscopy

In semi-crystalline polymers, the longitudinal acoustic vibrations propagate along regular molecular segments like along the elastic rods. The chain vibrations of this kind are called LAM. Owing to their efficient interaction with light, these modes produce specific bands in the low-frequency Raman spectra. It should be stressed that the linearity of the chain is a necessary condition of the propagation of LAM since there appear to be transverse oscillations in chain-breaking points. Local redistribution of the vibrational energy in favor of gaining the transverse acoustic modes in the locations of 'defect points' leads to the effective attenuation of the longitudinal mode.

The LAM frequency (ω_L) varies inversely with straight chain length (L). In the course of the polymer processing, treatment and utilizing, some effects of the structural transformation, including the decomposition of macromolecules, might take place. A rupture of straight chain or a *trans*-to-*gauche* transition in it (that is a formation of two shorter straight pieces of the same molecule) cause the appearance of two LAM localized in these adjacent pieces. The ratio between frequencies (ω_{L1}, ω_{L2}) of modified modes will be equal to the inverse length ratio ($L2/L1$) of newly formed SCS:

$$\omega_{L1}/\omega_{L2} = L2/L1 \tag{1}$$

Generally, the length of regular sequence between chain-ends and/or defects (*gauche*-conformers, points of branching) is related with the LAM frequency as [16]:

$$L = (2c\omega_L)^{-1} \times (E/\rho)^{1/2} \tag{2}$$

where c is the speed of light; ρ is the density, and E is the Young's modulus. The frequency of the LAM band maximum allows one to calculate with the help of Eq. (2) the most probable length of the straight segments; as a rule, this is close to the average crystal size in the chain direction.

As far as each SCS of a given length has its specific LAM frequency, the whole LAM band profile reflects the contribution of SCS of different lengths to the Raman intensity, or, in other words, the average-number SCS length distribution. However, owing to the dependence of the distribution function $F(L)$ not only on the number of oscillating SCS but also on the scattering efficiency of light and the population of vibrational energy levels, the original Raman spectrum is poor representative for aims of quantitative estimations, and $F(L)$ must be computed using a procedure based on the relation:

$$F(L) \propto [1 - \exp(-hc\omega/kT)]\omega^2 I(\omega) \tag{3}$$

Here, h is Plank's constant, k is Boltzmann's constant, and T is the absolute temperature; the expression $[1 - \exp(-hc\omega/kT)]$ characterizes the Boltzmann population of vibrational energy levels; $I(\omega)$ is the Raman intensity corrected for the Rayleigh scattering. To perform this correction, a background of the LAM spectrum in the vicinity of the central line must be approximated with an appropriate analytical function. In this work the central line was fitted to the Lorentzian which is well applicable for this procedure in the case of oriented polymers. The difference between the experimental spectrum and the approximating Lorentzian was taken as the effective intensity $I(\omega)$ in Eq. (3). A graphical illustration of this Raman data processing one can find in Ref. [17].

The value of the distribution function $F(L)$ calculated at a given L is proportional to the amount of the SCS with the length equal to L.

Using the LAM technique, one can detect the SCS both in crystallites and amorphous regions including the interfibrillar space, since the light scattering events of this kind are of one-dimensional character and not related to any three-dimensional structural units.

The LAM spectra excited with a 50 mW He–Ne laser were measured on a Raman spectrometer Spex Model 1401 equipped with a third monochromator.

The samples were placed into the laser beam in front of the collection optics of the spectrometer and axially deformed to produce a strain ε equal to 15%, that is approximately 0.8 of their ultimate strain (Fig. 1). Then the samples remained with their ends fixed, and the Raman spectra were periodically recorded until any spectral changes due to the stress relaxation were detectable.

The spectra were recorded in 90° geometry using XX light polarization, and with the film axis collinear to X direction. The measurements were carried out in the spectral range 6–30 cm^{-1} where the light scattering on longitudinal acoustic vibrations propagating along helical molecules yields a highly polarized band.

The acquisition time of the Raman measurement was 15 min.

3. Results

3.1. Broken bonds

The IR transmission spectra recorded prior to and after the stress application are shown in Fig. 2 in the range of absorption of chain-breakage products. Very low absolute intensity of the bands at 1640 and 1742 cm^{-1} is due to extrinsic character of the groups C=CH_2 and CH_2–CH=O which are absent in the repeating unit of i-PP macromolecules. However, one can see the increase of the intensities of the bands in as-strained samples. The calculated increments of the Lambert–Beer coefficient for both bands indicated are given in Table 1.

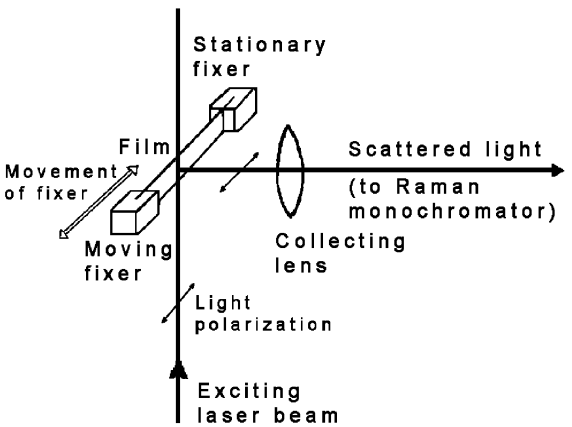

Fig. 1. A scheme of excitation of the Raman spectrum from the strained polymer film.

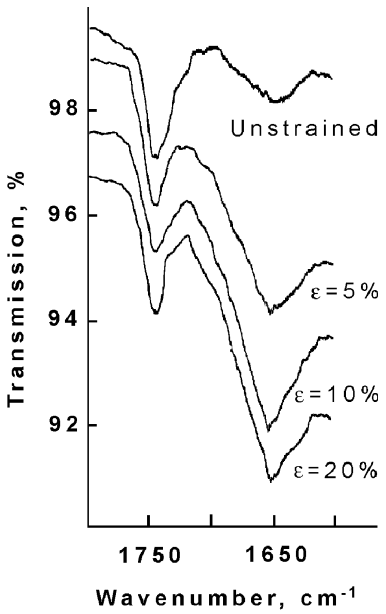

Fig. 2. IR transmission spectra in the range of the the bands at 1640 and 1742 cm^{-1} recorded prior to and after the straining the original sample. The strain values are shown near the spectra. To better indicate the difference between spectra, those of strained sample are shifted down the vertical axis.

3.2. SCS length distribution

Fig. 3 shows the low-frequency Raman spectra of the film recorded before straining and on subsequent stages of the stress relaxation. The computed from them functions $F(L)$, that is the SCS lengths distributions, are given in Fig. 4.

The spectra of heat-treated samples and corresponded functions $F(L)$ are shown in Figs. 5 and 6, respectively. To make more informative the changes in the SCS length distribution occurred as a result of strain and stress relaxation, the profiles $F(L)$ were convoluted into a set of three Lorentz components corresponding to three distinguishable features in the distribution function of the both samples. In unstrained, unheated sample the SCS length distribution is, in fact, bimodal with the peak positions at $L = 70$ Å and $L = 115$ Å. After straining the sample, the amplitude of the 115 Å peak decreases dramatically but then its integral value gradually grows

Table 1
The increment of the Lambert–Beer coefficient ($\Delta\alpha$) of the IR bands at 1742 and 1655 cm^{-1} in strained i-PP films

Polymer	Treatment	$\Delta\alpha$ (cm^{-1})	
		1742 cm^{-1}	1655 cm^{-1}
i-PP	Unstrained ($\varepsilon = 0$)	0	0
	$\varepsilon = 5\%$	5 ± 1	19 ± 2
	$\varepsilon = 10\%$	7 ± 1	30 ± 2
	$\varepsilon = 20\%$	17 ± 2	39 ± 2
i-PP, annealed	Unstrained ($\varepsilon = 0$)	29 ± 2	9 ± 1
	$\varepsilon = 20\%$	48 ± 2	10 ± 1

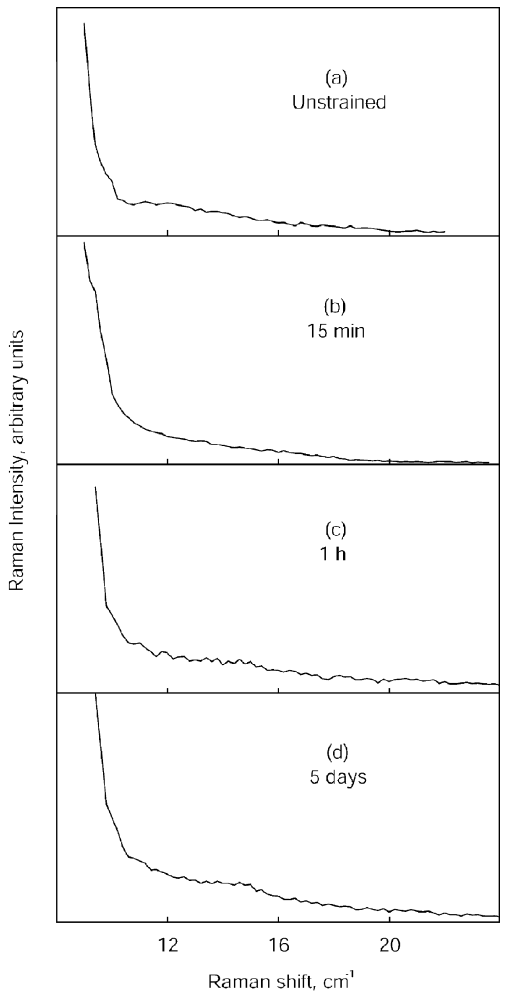

Fig. 3. Low-frequency Raman spectra in the frequency range of LAM bands. Original sample.

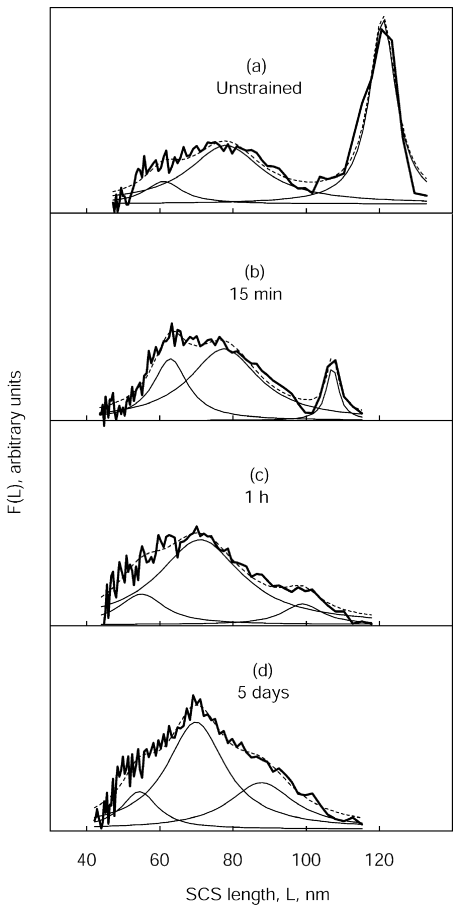

Fig. 4. The calculated SCS length distributions. Original sample.

again during subsequent strain exposition. This latter increase is accompanied by the broadening of the peak and its shift to lower lengths. The position of the main broad peak remains unchanged during the entire period of stress relaxation. In addition, a third weak-amplitude peak at ~50 Å appears after loading the sample.

Although the evolution of the distribution function during the stress relaxation in the annealed sample is lower expressive than that in the original sample, the main trends are the same. It is seen from the comparison of Figs. 4 and 6 that the behavior of each analytical component in the annealed sample is similar to the behavior of its counterpart in the original sample. Moreover, the final SCS length distributions in both relaxed samples are quite similar. Consequently, the annealing under the given conditions disturbs the ensemble of the SCS situated in non-folded chains but does not affect general trends in the SCS rearrangement during stress relaxation.

The annealing leads to the transformation of the bimodal SCS length distribution observed in unheated, unstrained sample to an asymmetric profile. The convolution procedure helps to separate three peaks situated at ~100, 70, and 50 Å (in stressed sample). One can see that the maximum of the distribution function in the annealed sample coincides with the position of the broader feature in the $F(L)$ profile of the original sample. Since the applied temperature regime of annealing (130 °C) could not cause the recrystallization in highly oriented i-PP, the broad peaks at 70 Å in both samples we attribute to the SCS in folded molecules.

As regards the narrow $L = 115$ Å peak in the original sample as well as the broad $L = 100$ Å component in the annealed sample, one should conclude that these features originate from a fraction of unstable 'non-crystalline' SCS highly sensitive both to the strain relaxation and heat treatment.

It is also worthy to notify the presence of well-pronounced small-amplitude features at $L = 50$ Å in both stressed/relaxed samples. Their amplitudes increase with the relaxation time. Taking into account the above given IR data which evidence the bond-breakage in strained films, we assign the peak at ~50 Å to of the 'debris' of the longer SCS broken during the stress relaxation. The permanent

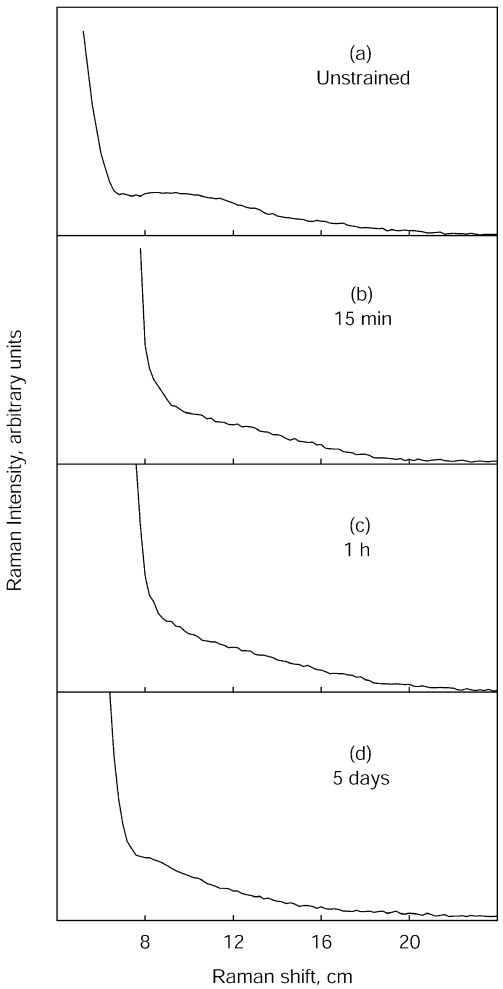

Fig. 5. Low-frequency Raman spectra in the frequency range of LAM bands. Annealed sample.

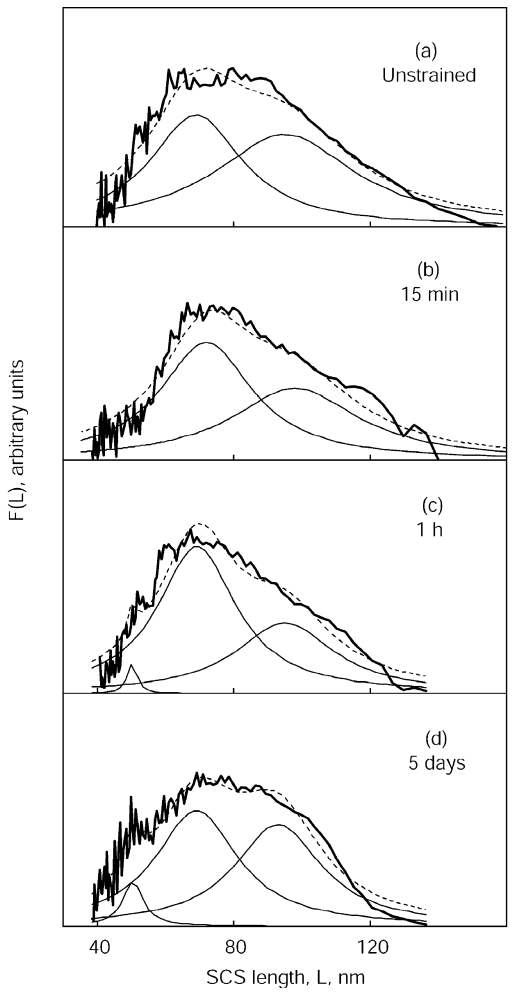

Fig. 6. The calculated SCS length distributions. Annealed sample.

chain-straightening process in the amorphous regions of strained samples also could contribute to this peak.

3.3. Mechanical tests

The strain–stress (σ versus ε) curves are shown in Fig. 7(a). Fig. 7(b) presents the E_t versus ε dependencies calculated from the σ versus ε curves (here $E_t = \partial\sigma(\varepsilon)/\partial\varepsilon$ is the tangent modulus [18]). The values of tangent modulus decrease at constant-rate straining of both the original and annealed samples.

The samples were strained up to $\varepsilon = 15\%$ and then left for relaxation for 15, 60 min and 5 days. On the end of each of these time periods, the straining procedure was recontinued after the Raman measurements, and the tangent moduli were measured. In Fig. 8, one of these stress–strain curves is depicted with explaining the experimental schedule of stepwise relaxation.

The values of the tangent moduli measured at various

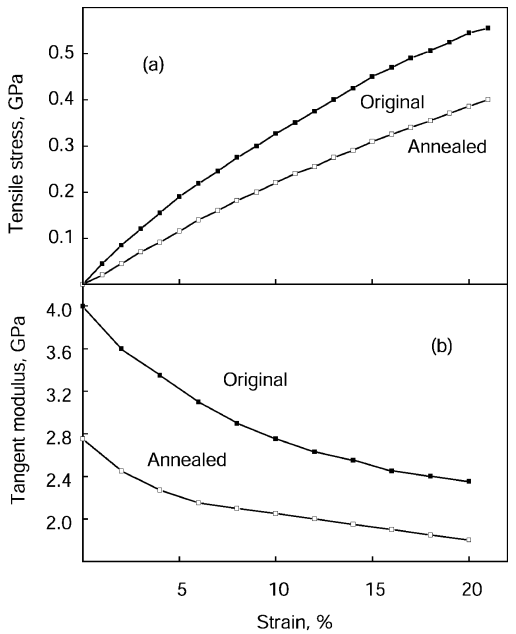

Fig. 7. Tensile stress (a) and tangent modulus (b) versus strain for the original and annealed samples.

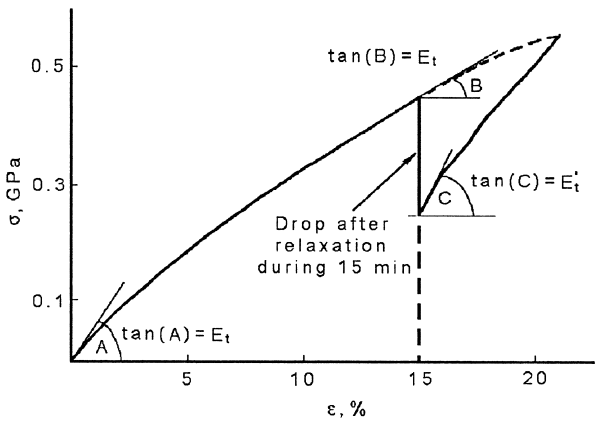

Fig. 8. An example of the stress–strain curve obtained with an interruption of straining at $\varepsilon = 15\%$ for relaxation during 15 min. Original sample.

stages of the samples' history (curves not presented) are collected in Table 2.

4. Discussion

The most intriguing result of the low-frequency Raman study is connected with the prominent feature at 115–100 Å in the SCS length distributions. Its small width in the original sample, on the one hand, and its strong response to the heat and mechanical treatment, on the other hand, evidence the presence of a particular fraction of the SCS whose average length exceeds the thickness of crystal cores (L_c). This peak cannot be ascribed to the taut-tie molecules (TTM) linking neighboring crystallites. Really, the length of the TTM is a sum of lengths of, at least, two crystallites and an amorphous layer situated between them. Under supposition that the peak at $L = 70$ Å in all samples belongs to folded molecules of length equal to L_c, the TTM must be longer than $2L_c = 2 \times 70 = 140$ Å. One can see that the lengths of the longest detected SCS (Figs. 4 and 6) are smaller than the suggested TTM length.

Table 2
Tangent modulus at various stages of sample treatment

Sample, i-PP	Treatment	Tangent modulus: E_t, E'_t (GPa)
Original	Unstrained[a]	$E_t = 4.0 \pm 0.1$
	Strained, $\varepsilon = 15\%$	
	As-strained	$E_t = 2.50 \pm 0.10$
	Stress relaxation during 15 min	$E'_t = 5.80 \pm 0.15$
	Stress relaxation during 1 h	$E'_t = 6.00 \pm 0.15$
	Stress relaxation during 5 days	$E'_t = 6.50 \pm 0.15$
Annealed	Unstrained[a]	$E_t = 2.70 \pm 0.10$
	Strained, $\varepsilon = 15\%$	
	As-strained	$E_t = 1.80 \pm 0.10$
	Stress relaxation during 15 min	$E'_t = 4.80 \pm 0.10$
	Stress relaxation during 1 h	$E'_t = 5.20 \pm 0.15$
	Stress relaxation during 5 days	$E'_t = 5.50 \pm 0.15$

[a] Initial tangent modulus was measured under condition $\varepsilon \to 0$. For explanation of denotations see Fig. 8.

To facilitate the interpretation of the spectroscopic results, it is instructive to establish a correlation between the changes in the SCS length distribution function and the rigidity under the same conditions. Such approach is justified by the great significance of the chain-straightening process in formation of the mechanical properties of semicrystalline polymers [19].

First of all, the transformation of narrow $L = 115$ Å peak to broad shoulder at ~ 100 Å as a result of annealing is accompanied by the decrease of the tangent modulus from 4.0 to 2.7 GPa. The decrease of the elastic modulus in injected mould i-PP after annealing conducted under similar

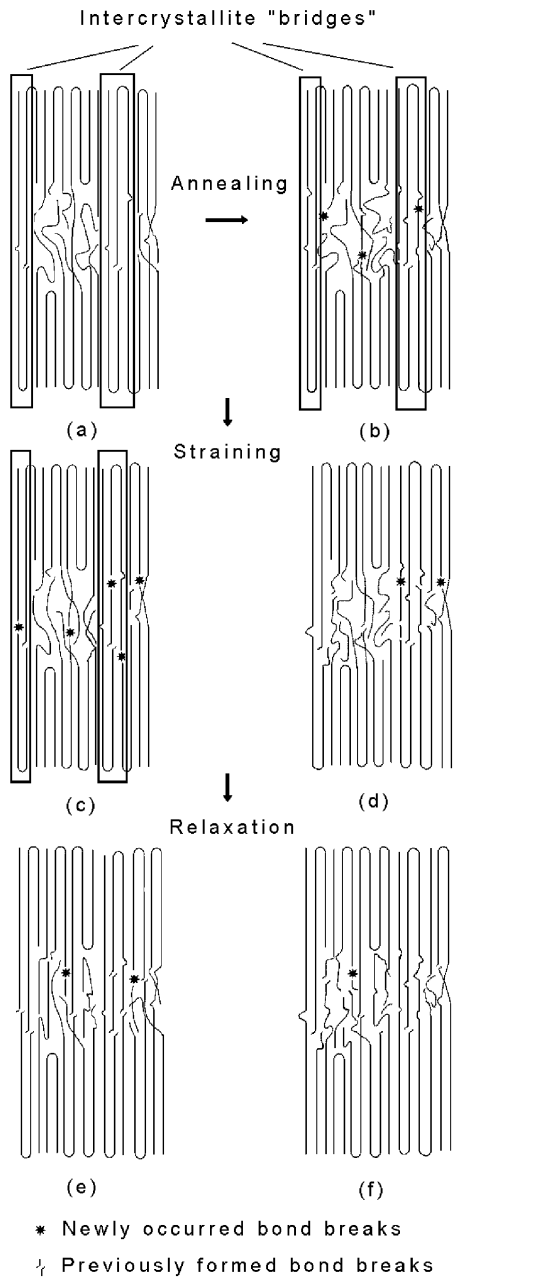

Fig. 9. Transformation of the intercrystallite structure in the oriented i-PP film at various stages of material processing.

conditions was also reported by Drozdov and Christiansen [9]. This effect can be explained by coiling of a part of particular fraction of longest SCS during the heat treatment (Fig. 9(a) and (b)); this is supported by the significant value of measured shrinkage ratio (6%); the thermal destruction (bond-breakage) also enable to give its contribution to this effect. The decay of the longest SCS reduces the fibril stiffness with decreasing the value of E_t.

A dramatic decrease of the $L = 115-100$ Å peak intensity in a short time after loading coincides with a drop of the tangent modulus from 4.0 to 2.5 GPa and from 2.7 to 1.8 GPa in original and annealed samples, respectively. Simultaneously, a feature at ~50 Å (belonging, as suggested, to short-length SCS resulting from ruptures of longer straight chain) becomes well-pronounced in the SCS length distributions. We conclude again that the decrease of the fraction of the SCS related to the $L = 115-100$ Å peak reduces the structure rigidity.

During the isometric stress relaxation, the amplitude of this peak gradually increases with a drift of its position in direction of smaller lengths. Simultaneously, the amplitude of the peak at ~50 Å grows. In terms of the structure modification, the chain-straightening process is accompanied with multiple chain-breaking events. From the persisting growth of the tangent moduli during all the period of the stress relaxation (Table 2) one can deduce the prevailing role of the ordering process even if it is affected by limited polymer decomposition.

In many works appeared from seventies up to now, Ward and co-workers [16,19,20–23] promoted their postulate that the Young's modulus of semicrystalline polymers is uniquely related to the draw ratio, irrespective of their initial morphology. They put forward a bridge model [21] implying the existence of 'long crystals' linking crystallites in highly oriented samples. In terms of the molecular structure, the intercrystallite bridges are composed of the regularly arranged SCS passing from one folded crystal to another through an amorphous region. In accordance with the conjecture of Ward and co-workers [21], the growing population of the TTM provides the increase of the structural rigidity with the increase of the draw ratio. A previous LAM study of highly oriented gel-derived PE fibers [24] evidenced the presence of TTM passing through 2–4 subsequent crystallites.

However, we failed to detect TTM in our highly oriented i-PP samples.

The behavior of the peak situated at $L_c < L < 2L_c$ becomes comprehensive if one admits that the 'crystalline bridges' between folded crystallites contain a noticeable amount of defects (Fig. 9(a)). Local ruptures or newly appeared conformer insertions in the SCS passing through amorphous layers reduce the average length of the bridging SCS to $L < 2L_c$ but isolated defects do not affect significantly the stiffness of fibrils. The annealing stimulates the chain-coiling and thermal destruction processes which introduce additional defects in 'long' helical molecules that contribute to the $L_c < L < 2L_c$ peak (Fig. 9(b)). This leads to broadening of the SCS length distribution in the 'bridges'.

The mechanical destruction in the stressed sample acts in a similar manner but in spite of the coiling events, the degradation of 'bridges' is resulted from the bond breakage (Fig. 9(c) and (d)). At the same time, the stress relaxation (in contrast to the thermal relaxation) is accompanied by the straightening of individual chain-segments throughout the amorphous regions. The intercrystallite space transforms to the partially ordered structure composed of various-lengths SCS with coiled insertions (Fig. 9(e) and (f)). In contrast to stressed PE whose linear macromolecules slide readily through crystallites with formation of TTM [24], the force-induced uniaxial arrangement of helical chains in i-PP is accompanied with multiple chain ruptures preventing the formation of the defect-free intercrystallite 'bridges'. Individual defect 'bridges' existed in unstrained polymer degrade more and more, and gradually become 'dissolved' in so formed 'rigid amorphous phase' [9,24]. The increased values of tangent modulus in relaxed samples indicate the prevailing significance of the total amount of the SCS in the formation of the mechanical properties in comparison with the supramolecular elements of rigidity such as 'bridges' or 'bundles'. However, in the context of the bridge model [21], one can regard these modified intercrystallite space as a kind of bulk bridging structure.

5. Conclusion

The intercrystallite bridging structures in the oriented i-PP are formed by ordered SCS whose average length falls in the range $L_c < L < 2L_c$. The chain-breakage in stressed samples causes the reduction of the average length of the SCS involved in these quasi-crystalline entities with corresponded decrease of the tangent modulus.

The annealing of the oriented sample leads to decay of the ordered 'bridges' due to chain-coiling events throughout the intercrystallite regions but a significant amount of one-dimension $L > L_c$ stems remains in fibrils. The heating-induced decomposition of the bridges also affects the tangent modulus.

During the isometric stress relaxation in strained samples, the growing fraction of 'individual' SCS compensates the loss of three-dimensional bridging structures. The intercrystallite space transforms to the rigid amorphous phase composed of one-dimensional molecular stems with a wide length distribution. This quasi-ordered structure gains the rigidity of fibrils in relaxed samples as efficiently as the TTM or intercrystallite 'bridges' in as-drawn films or fibers.

Acknowledgements

K.T. acknowledges the support of the President Counsel of the Russian Federation ('Program of support of the

Principal Science School in Physics and Mechanics of Polymers and Material Science—Oriented Polymers, NS 1.9.03').

References

[1] Karger-Kocsis J, editor. Polypropylene an A–Z reference. Dordrecht: Kluwer Academic Publishers; 1999.
[2] Read BE, Tomlins PE. Polymer 1997;38:4617–28.
[3] Viville P, Daoust D, Jonas AM, Nysten B, Legras R, Dupire M, Michel J, Debras G. Polymer 2001;42:1953–67.
[4] Aboulfaraj M, G'Sell C, Ulrich B, Dahoun A. Polymer 1995;36: 731–42.
[5] Labour T, Gauthier C, Séguéla R, Vigier G, Bomal Y, Orange G. Polymer 2001;42:7127–35.
[6] Mendoza R, Régnier G, Seiler W, Lebrun JL. Polymer 2003;44: 3363–73.
[7] Wiyatno W, Pople JA, Gast A, Waymouth RM, Fuller GG. Macromolecules 2002;35:8488–97.
[8] Drozdov AD, Christiansen Jde C. Eur Polym J 2003;39:21–31.
[9] Drozdov AD, Christiansen Jde C. Polymer 2002;43:4745–61.
[10] Schultz JM. Polymer materials science. Englewood Cliffs, New York: Prentice Hall; 1974.
[11] Ciferri A, Ward IM, editors. Ultra-high modulus polymers. London: Applied Science Publishers; 1977.
[12] Sakurada I, Ito T, Nakamae K. In: Stein RS, Onogi S, editors. US–Japan seminar in polymer physics. New York: Interscience; 1966. p. 75.
[13] Peterlin A. J Appl Phys 1979;50:838–46.
[14] Bassett DC, Olley RH. Polymer 1984;25:935–43.
[15] Rabolt JF, Fanconi BJ. Polym Sci: Polym Lett Ed 1977;15:121–7.
[16] Capaccio G, Crompton TA, Ward IM. J Polym Sci: Polym Phys Ed 1976;14:1641–58.
[17] Pakhomov PM, Khizhnyak S, Reuter H, Galitsyn V, Tshmel A. Polymer 2003;44:4651–4.
[18] Schultze-Gebhardt F. Faserforsch und Textiltechn 1977;28:467–75.
[19] Ciferri A, Ward IM, editors. Ultra-high modulus polymers. London: Applied Science Publishers; 1977.
[20] Capaccio G, Wilding MA, Ward IM. J Polym Sci: Polym Phys Ed 1981;19:1489–92.
[21] Al-Hussein M, Davies GR, Ward IM. Polymer 2001;42:3679–86.
[22] Amornsakchai T, Bassett DC, Olley RH, Al-Hussein MOM, Unwin AP, Ward IM. Polymer 2000;41:8291–8.
[23] Amornsakchai T, Olley RH, Bassett DC, Unwin AP, Ward IM. Polymer 2001;42:4117–26.
[24] Pakhomov PM, Khizhnyak S, Galitsyn V, Ruhl E, Vasil'eva V, Tshmel AJ. Macromol Sci–Phys 2002;B41:229–40.